Vadose Zone Journal

Special Section: TOUGH2

Modeling Soil Moisture Processes and Recharge under a Melting Snowpack

Alan L. Flint,* Lorraine E. Flint, and Michael D. Dettinger

Recharge into granitic bedrock under a melting snowpack is being investigated as part of a study designed to understand hydrologic processes involving snow at Yosemite National Park in the Sierra Nevada Mountains of California. Snowpack measurements, accompanied by water content and matric potential measurements of the soil under the snowpack, allowed for estimates of infiltration into the soil during snowmelt and percolation into the bedrock. During portions of the snowmelt period, infiltration rates into the soil exceeded the permeability of the bedrock and caused ponding to be sustained at the soil–bedrock interface. During a 5-d period with little measured snowmelt, drainage of the ponded water into the underlying fractured granitic bedrock was estimated to be 1.6 cm d^{-1}, which is used as an estimate of bedrock permeability. The numerical simulator TOUGH2 was used to reproduce the field data and evaluate the potential for vertical flow into the fractured bedrock or lateral flow at the bedrock–soil interface. During most of the snowmelt season, the snowmelt rates were near or below the bedrock permeability. The field data and model results support the notion that snowmelt on the shallow soil overlying low permeability bedrock becomes direct infiltration unless the snowmelt rate greatly exceeds the bedrock permeability. Late in the season, melt rates are double that of the bedrock permeability (although only for a few days) and may tend to move laterally at the soil–bedrock interface downgradient and contribute directly to streamflow.

Abbreviations: HDP, heat dissipation probe; TDR, time domain reflectometry.

Infiltration of water into bedrock in mountainous terrain represents a significant portion of recharge in the western United States, especially under conditions of a melting snowpack (Wilson and Guan, 2004; Flint et al., 2004). Under anticipated increases in air temperature associated with global warming, snowmelt processes and the associated runoff in the Sierra Nevada Mountains are likely to occur earlier in the springtime (Dettinger et al., 2004), with uncertain implications regarding recharge. Developing a better understanding of the processes contributing to mountain block recharge under these conditions is deemed prudent (Earman et al., 2006).

The conceptual model of infiltration into bedrock was described by Flint et al. (2004) as resulting from water percolating through a shallow soil column at a rate exceeding that of the underlying bedrock permeability, ponding at the bedrock interface, and penetrating the bedrock at a rate equivalent to the permeability of the fractured bedrock. Use of a basin-scale water-balance model (Flint et al., 2004) that accounts for melting snow, the physical characteristics of a location dominated by the granitic bedrock present throughout much of the Sierra Nevada, and shallow soils generally results in calculations indicating a higher potential for runoff than in-place recharge into the bedrock (Flint et al., 2004). This process is strongly controlled by the bulk bedrock permeability, the nature of the matrix and fracture properties reflected in the bedrock moisture retention characteristics, and the rate of snowmelt. The contribution of bedrock infiltration was shown in a small headwater catchment by Kosugi et al. (2006), who illustrated that saturated flow from overlying soil into weathered granite was the dominant hydrologic process at the soil–bedrock interface. This study supports the conceptual model of Flint et al. (2004) that regards the soil thickness as one of the most important influences on the relative proportion of bedrock infiltration and saturated lateral flow.

Catchment-scale analyses of water budget have been used to estimate rates of bedrock infiltration (Terajima et al., 1993; Anderson et al., 1997). However, few local-scale field measurements of all of the various processes have been made that allow for estimation of the bulk bedrock permeability (combination of matric and fracture permeability) and when accompanied by detailed numerical investigations, provide a means to glean additional understanding of how the processes of snowmelt, soil moisture flow, ponding, bedrock flow, and redistribution operate in this complex system.

The USGS, working with the Scripps Institution of Oceanography and the California Cooperative Snow Surveys, has established a research field site located in Yosemite National

U.S. Geological Survey, 6000 J St., Sacramento, CA, 95819-6129.
Received 15 Sept. 2006. *Corresponding author (aflint@usgs.gov).

Vadose Zone J. 7:350–357
doi:10.2136/vzj2006.0135

Park at a California Department of Water Resources snow-instrumented station on the western boundary of the park at Gin Flat to study soil moisture processes under the accumulation and melting of snow (Fig. 1). This research is part of the California Energy Commission's Climate Change Center's research program to understand how climate change will influence California's future economic, social, and natural systems.

The established field site hosts a variety of instruments to measure turbulent heat and vapor fluxes, soil moisture and temperature, and snowpack temperatures. Specifically, the soil measurements of matric potential, water content, and temperature are used to develop conceptual models of the interaction between the soil and snowpack. The measurements are accompanied by calculations of snowmelt, on the basis of snow pillow measurements, to provide properties and boundary conditions for a numerical model to elucidate the relative importance of the processes and to test hypotheses regarding soil moisture drainage and bedrock infiltration. Overall, the study will help develop an understanding of the water balance between the atmosphere, snowpack, soil moisture, drainage, recharge, and runoff.

Methods

Measurements

For the purposes of investigating the processes occurring in the snowpack, instruments were installed to measure the temperature and volume of the snow, as well as all of the associated meteorological components (e.g., solar radiation, net radiation, evapotranspiration, sublimation). An array of temperature loggers (~0.25°C resolution) were suspended approximately every 15 cm from 3 to 248 cm above the soil surface with one temperature logger buried −12 cm below the surface. Acoustic vertical-distance sensors operated by University of California at Merced provided snow thickness data (Bob Rice, personal communication, 2004). Adjacent to (within 10 m) the aboveground snow instruments, soil instrumentation was installed in the 76-cm deep, loamy sand, overlying fractured granite (Fig. 2). Measurements were made at 4-h intervals from the fall of 2002 to March 2004, then changed to hourly intervals until the fall of 2004, and are used to illustrate the subsurface processes associated with the 2004 springtime snowmelt.

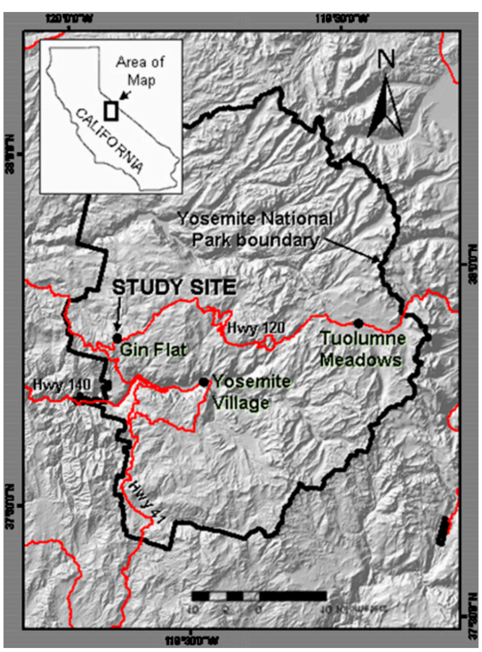

FIG. 1. Map of study location in Yosemite National Park, central Sierra Nevada Mountains.

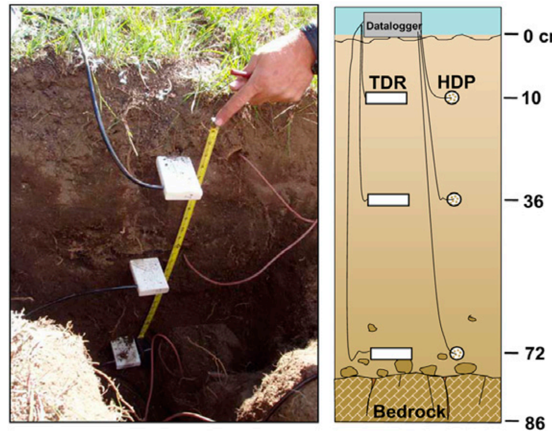

FIG. 2. Time domain reflectometry (TDR) and heat dissipation probes (HDP) at three depths in shallow soil above granitic bedrock.

A series of time domain reflectometry (TDR; Model CS 615 and 616, Campbell Scientific, Inc., Logan, UT) probes were installed at 10, 36, and 72 cm below the surface to measure soil water content. Alongside the TDR probes were heat dissipation probes (HDPs) calibrated to an extended range (Flint et al., 2002) that measure soil matric potential and soil temperature (Fig. 2). During instrument installation, bulk soil samples and soil cores were taken for measurements of physical and hydrologic properties. Laboratory measurements of bulk density (using core method; Grossman and Reinsch, 2002), particle density (using helium pycnometry; Flint and Flint, 2002a), porosity (calculated from bulk density and particle density; Flint and Flint, 2002b), and moisture retention characteristics (using pressure pots; Dane and Hopmans, 2002) were conducted. Thermal conductivity and heat capacity were measured on soil samples in the laboratory using the dual-probe heat pulse method (Kluitenberg, 2002).

Model Development

Using the numerical simulator TOUGH2 (Pruess et al., 1999), a two-dimensional model was developed using measured soil properties with three soil layers, 25, 30, and 20 cm thick (Table 1), and one bedrock layer (25 cm thick). The upper bound-

TABLE 1. Results of laboratory measurements on soil samples.

	Layer 1	Layer 2	Layer 3
Hydrologic properties			
Depth (cm)	25	30	20
Bulk density (g cm^{-3})	1.52	1.53	1.39
Porosity (cm^3 cm^{-3})	0.436	0.433	0.486
Grain density (g cm^{-3})	2.7	2.7	2.7
Gravel (% of total soil)	16	22	24
Organic matter (% of total soil)	7	5	5
Sand (% of fines)	85	86	88
Silt (% of fines)	10	8	8
Clay (% of fines)	5	6	4
van Genuchten alpha (1 Pa^{-1})	1.37E-04	1.05E-04	2.43E-04
van Genuchten m	0.3038	0.3136	0.3162
Thermal properties			
Thermal conductivity (W m^{-1} K^{-1}; soil VWC = 0.10 cm^3 cm^{-3})	1.17	1.17	1.17
Specific heat (kJ kg^{-1} K^{-1})	1.15	1.15	1.15

ary condition consisted of a specific flux identified on the basis of the variable snow melt and the lower boundary condition was a specified matric potential to maintain drainage below the bedrock layer. Water moved from the soil into the bedrock layer only when the soil above was nearly saturated. Grids consisted of 5-cm-thick layers with the model domain being 1 m deep × 10 m wide with a 5% topographic slope, estimated on the basis of general site conditions, to evaluate the potential for lateral flow at the soil-bedrock interface. Two scenarios were investigated with the two-dimensional model: seasonal processes at three depths for 3 mo during the snowmelt period, and hourly melt and drain processes at the beginning of snowmelt. The hourly timing of snow melt was not known but was assumed to ramp up then down between 10:00 a.m. to 7:00 p.m. by adding and subtracting increments of approximately 0.025% of the total daily melt per hour. On each day of melt at 10:00 a.m., an initial flux of 0.05% was assigned, which was incremented at 11:00 a.m. to 0.075% so that by 2:00 p.m. it was 0.15% The flux at 3:00 p.m. was also set to 0.15% which was then ramped down until 7:00 p.m., which had a flux of 0.05% Snowmelt was stopped after that until the next day, when the process was started over again at 10:00 a.m. with a new total daily melt.

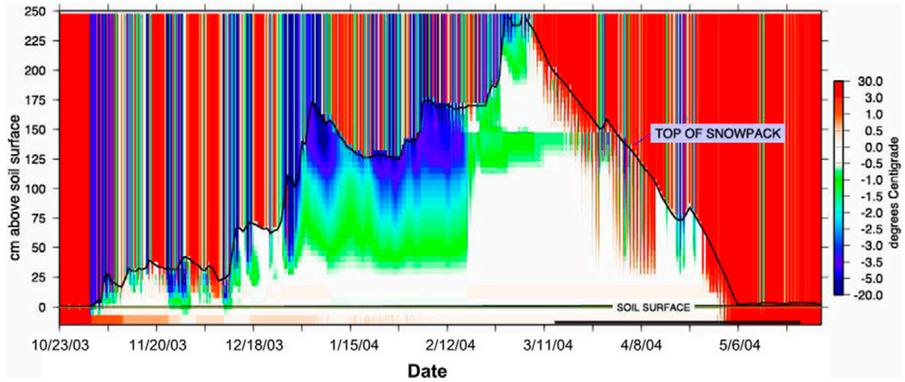

Fig. 3. Half-hourly snow and air temperatures, and snow depths, during winter 2003–2004 at Gin Flat.

The only property that could be adjusted in a calibration process to match simulated data with measured data was the bulk bedrock permeability. This was changed iteratively until the drainage profile in the model matched the measured data.

Results and Discussion

Laboratory Measurements

Soil samples were measured to provide hydrologic and thermal properties for each of the three soil layers (Table 1). Soil water content measurements were made periodically to help develop field-specific calibration equations for the TDR probes; however, site access problems (roads closed due to snow) only allowed for measurements during relatively dry periods. An average soil permeability of 400 cm d^{-1}, estimated from textural properties using Rosetta (Schaap et al., 2001), was used for the numerical model. Rock properties were estimated from literature values and modified to match summer dry equilibrium conditions for the soil with a porosity of 0.04 cm^3 cm^{-3}, grain density of 2.7 g cm^{-3}, van Genuchten alpha of 2.43E-4 (1 Pa^{-1}), and van Genuchten m of 0.3162. Bulk bedrock permeability was determined iteratively using computer simulations.

Field Data

Snow persisted at the site from about 1 Nov. 2003 to early May 2004. Snow accumulation and compaction can be seen to persist until early March 2004. Snow accumulation occurred during below-freezing snow events, with snow compaction (and sublimation) occurring during above-freezing events (Fig. 3). The cold air temperature from late December 2003 and intermittently until mid-February kept the upper meter of the snowpack considerably colder than the approximately 0°C in the bottom 25 cm that persisted through the entire period. Around mid-February, cloudy conditions and warm temperatures heated the snowpack to near 0°C conditions, which is where most of it remained until the melt was over in early May. Estimates of snowmelt and input to the soil column were made from 14 March to 15 May 2004 (Fig. 4). The day-to-day changes in daily mean snow-water content values at the Gin Flat snow pillow were computed (by subtracting each day's mean content from the mean content the day before). On most days, this change was considered to be the infiltration rate. On the few spring days when precipitation was recorded at Gin Flat and the Hetch Hetchy manual gage, if the snow water content at the snow pillow stayed the same or declined, the precipitation value from the Gin Flat gage was added to the snow-water content change to estimate the total infiltration rate for that day. On wet days when the snow-water content at the snow pillow increased, the precipitation rate was reduced by the gain in snow-water content, and the remainder was assumed to infiltrate.

Volumetric soil-water content is shown in Fig. 5 for three depths. Water content was the highest for the 72-cm depth, where it reached saturation under ponded conditions in early April. Initial evaluation of the data suggested that the water content at the 10-cm depth seemed low but could possibly be explained as a soil under steady-state conditions with melting

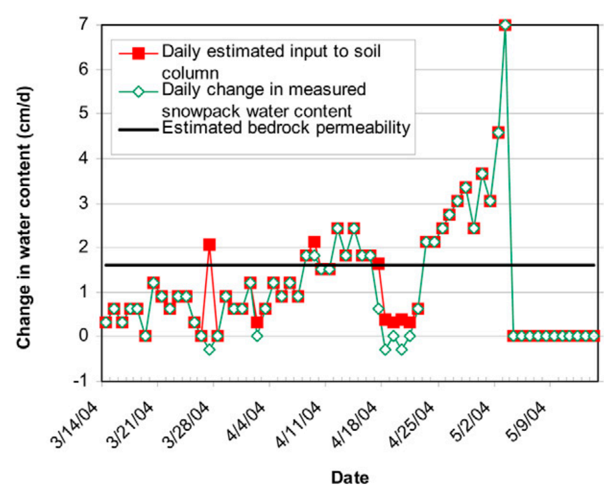

Fig. 4. Estimated daily changes in snow water content, daily inputs to soil column, and bedrock permeability at Gin Flat.

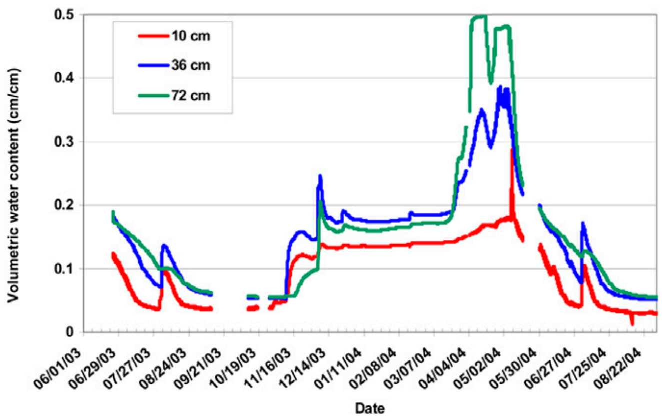

Fig. 5. Volumetric soil water content for June 2003 to September 2004 at three depths.

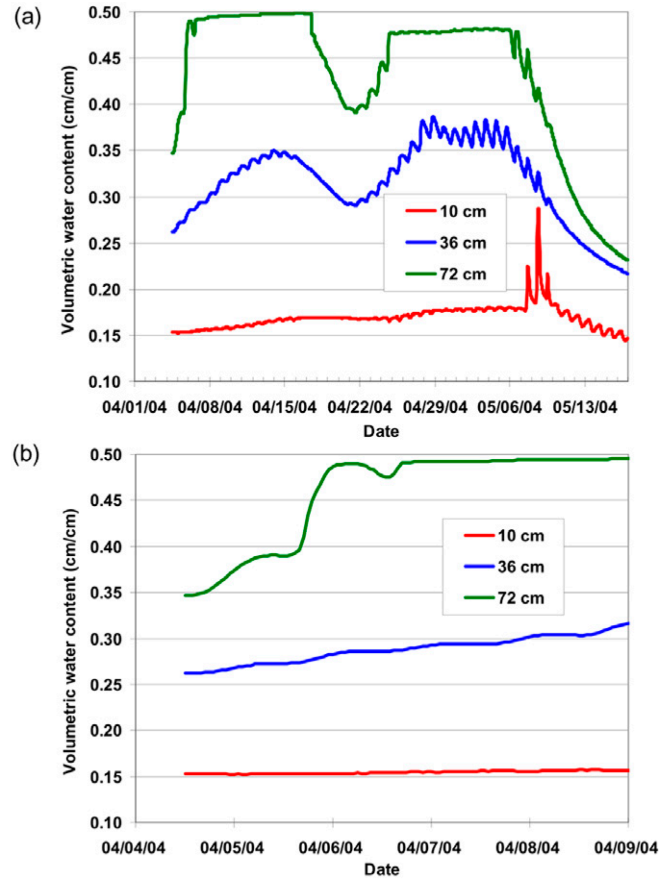

Fig. 7. Detailed soil water content for springtime snowmelt for (a) the month of April 2004 and (b) for 4–9 Apr. 2004.

snow (water content becomes constant under steady-state gravity drainage). Numerical modeling suggests possible measurement errors, which are discussed later. At the maximum water content, after snowmelt in April, the soil profile contained more than 28 cm of water; in September, at the minimum water content, the soil profile contained about 4 cm of water (Fig. 6).

Hourly soil moisture measurements for 6 wk in April and May (Fig. 7a) illustrate daily fluctuations that resulted from nightly freezing of the snowpack and subsequent daytime snowmelt. The snowpack temperatures show the alternating melt and freeze as red and white bands of temperature over the snowmelt period (Fig. 3). The soil drained continuously as long as water was available, regardless of snow processes, but soil-water content fluctuated according to the drainage of snowmelt water in the soil each day.

Diurnal changes in water content of the soil profile resulted from infiltration into the soil and can be seen in all three instrumented layers. Snowmelt was initiated around 14 March (Fig. 3 and Fig. 4) but at a rate lower than the estimated permeability of the bedrock (Fig. 4). As the snow started and stopped melting diurnally, small pulses of water increased the water content at 10 and 36 cm, and then decreased as the water drained away. The 72-cm depth shows similar patterns until it became saturated, and even then there were small fluctuations near saturation. The sequence continued until a large cold front resulted in the discontinuation of diurnal melting between 18 and 23 April, which added new snow to the snowpack (Fig. 3). This was followed by

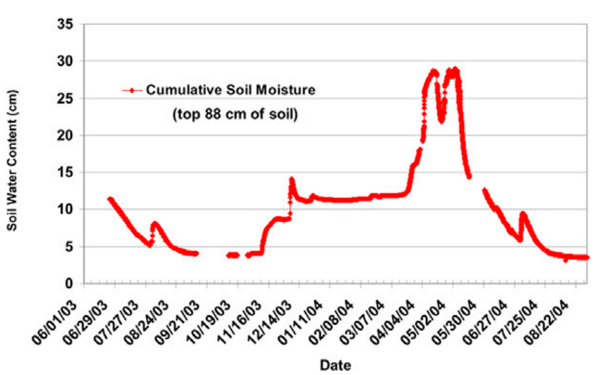

Fig. 6. Cumulative water content for entire soil profile for June 2003 to September 2004.

an increase in temperature, and the diurnal melt started again. Snow began melting again on 23 April, resulting in increased soil-water content. Calculations indicated that approximately 3.5 cm d^{-1} was draining into the 88-cm-deep soil, exceeding the permeability of the bedrock and causing ponding at the soil–bedrock interface (saturation at the 72-cm depth and near saturation at the 36-cm depth until the second week of May). Divergence from the estimated input to the soil column of 2.0 cm d^{-1} (Fig. 4) for that period may be due to the heterogeneity of the melting of the snowpack discussed earlier. Water was ponded and the soil was saturated at the 72-cm depth beginning 7 April (Fig. 7b). Hourly soil-water measurements indicate that melt water penetrated the soil column in less than 2 h. Soil matric potential is shown for the same three depths and supports the interpretation of saturated conditions as the bottom two depths reached −0.001 MPa (Fig. 6). The 36-cm depth likely had hysteretic conditions and air entrapment resulting in less than full saturation (indicated by the TDR data). This is noted by comparing Fig. 7a and 8 at the 36-cm depth between 6 March and 6 May 2004, which show water potential at or near saturation (indicated by the HDP). During April 18 to 23, which was a period of little snowmelt (0.3 cm d^{-1}), calculations on the basis of the slope of the declining water content between 18 and 23 April and between 5 and 16 May indicated that 1.6 cm d^{-1} (and up to 1.9 cm d^{-1}) of water infiltrated into the saturated bedrock. The drainage that occurred during that period can also be seen as a slight upward movement from saturation at the 36- and 72-cm depth around 20 March (Fig. 8). Calculations of changes in soil moisture indicated that

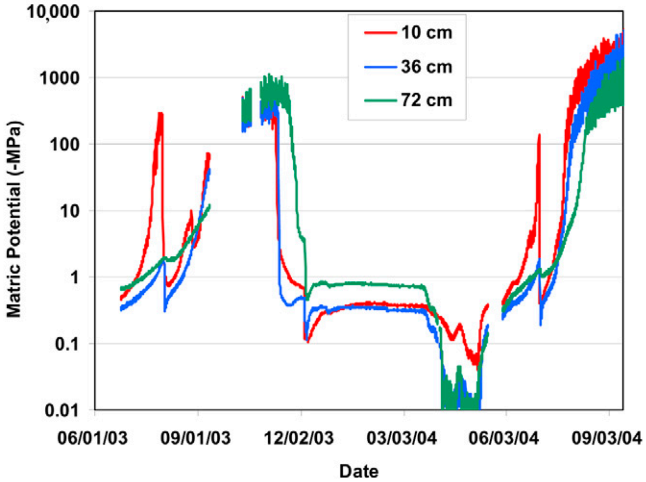

FIG. 8. Soil-water potential for June 2003 to September 2004 at three depths.

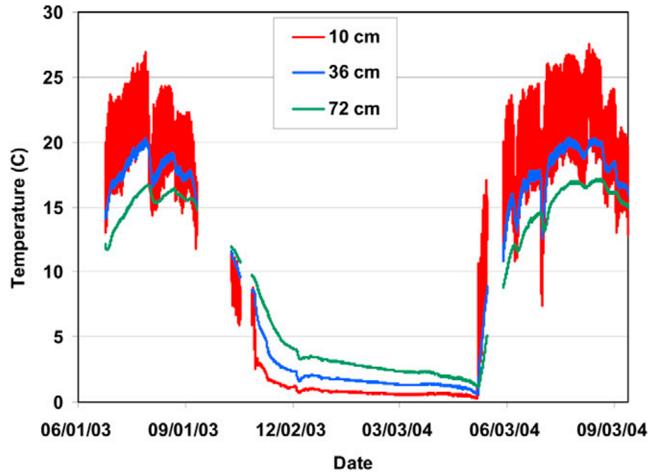

FIG. 10. Soil temperature for June 2003 through September 2004 at three depths.

there was approximately 36 cm of soil water storage capacity and approximately 28 cm of water stored at the maximum wetness during the study period.

Soil-water retention characteristics are shown in Fig. 9 for laboratory measurements and field measurements, illustrating possible hysteresis in the field observations, but also providing relative confirmation of laboratory measurements. The three soil depths are quite similar in their retention characteristics, with the exception of the 10-cm field data. It appears that the TDR data at 10 cm may be too low, causing a shift in the field water retention curve, which also suggests possible errors in the TDR measurement. The laboratory-derived water retention curves were used in numerical simulations.

Soil temperature measurements at the three depths (Fig. 10) illustrate when the site was snow covered as exemplified by the drop in temperature and lack of daily fluctuations. The end-of-spring snowmelt can be seen as a sharp rise in soil temperature beginning 9 May, accompanied by distinct daily temperature fluctuations, indicating lack of snow cover. The snowmelt at the snow pillow ended 4 d earlier (5 May 2004, Fig. 3). The soil-instrumented site is north of the snow pillow, with several trees potentially shading the snowpack, which may be why the snow persisted for four additional days. The slight heterogeneity in snowpack indicated by the differences in snowmelt over relatively short distances (less than 10 m between the soil instrumentation and snow pillow) also indicates that the snowmelt data used in the simulation (Fig. 4) may not be same as that above the soil instruments.

To test the hypothesis that the soil heat flux was contributing to the melting snowpack from below, soil heat flux was calculated from soil temperature measurements between the 10-cm and 36-cm depths and between the 36- and 72-cm depth (Fig. 11). Flux of heat moving upward from the ground into the snowpack, shown for the November to May period when the flux has no diurnal fluctuations, is approximately 5 to 10 W m^{-2}. This small heat flux is considered to be an insignificant contributor to snowmelt at this location.

Uncertainties in calculations of bedrock infiltration are a result of the uncertainty in local slope conditions that could impact heterogeneities in lateral flow at the soil–bedrock interface. If the site

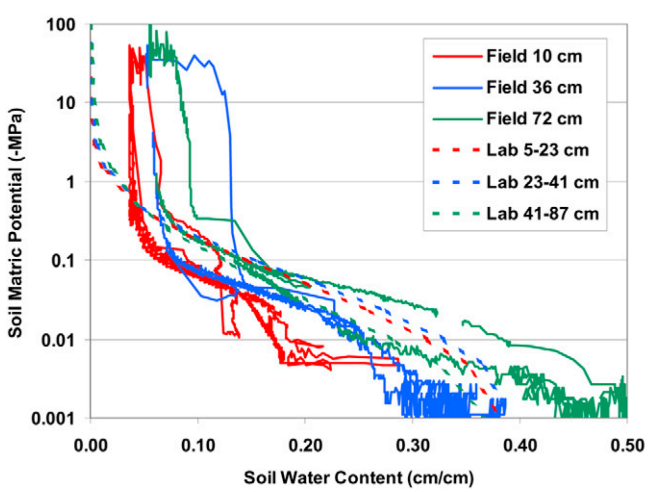

FIG. 9. Laboratory and field water retention curves for soil at three depths.

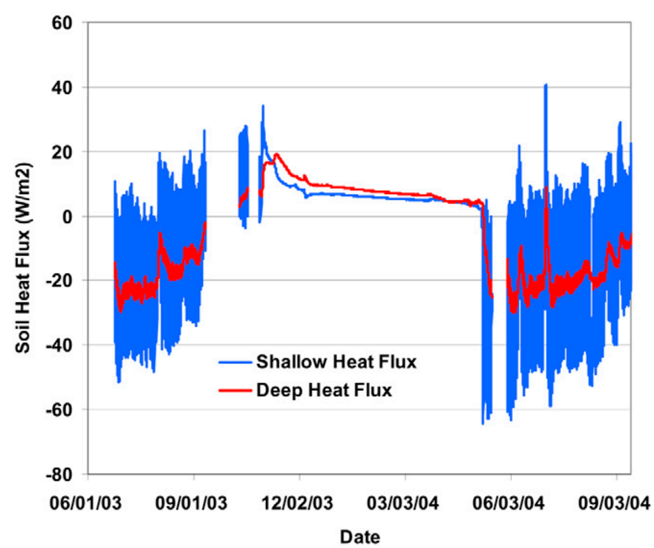

FIG. 11. Soil heat flux calculated from soil temperature measurements for shallow soil (10–36 cm) and deep soil (36–72 cm).

had a slight but consistent slope, lateral flow would enter the measurement domain at the same rate that it left, although increased flow from the vertical direction would cause a rise in the perched system. This would result in no net changes in water content at the 72-cm depth and provide a more accurate estimate of bedrock infiltration, assuming enough upslope water availability.

Model Results

Simulations were made with the two-dimensional model for a 3-mo period, 14 March through 14 May 2004, to simulate the snowmelt period (Fig. 12). The model shows reasonable agreement at the 72-cm depth but shows higher-than-measured water contents at 10 and 36 cm. It should be noted that the measured 10-cm data in Fig. 12 is not the same as that in Fig. 5. The measured HDP data for the 10-cm depth were converted to water content using the laboratory-measured water retention curve to replace the assumed bad TDR data from that depth (other instrument errors might cause the lack of fit between the model and measurements, but we do not have enough data to justify making additional changes using the HDP data at this time). It can be seen that model simulations mimic the melt and no melt (refreezing conditions, and then continued melt for the three soil layers for this period of time). Although there are mismatches between the simulated and measured data, we believe the process of ponding and draining at the bedrock interface is in reasonable agreement with the field data. When additional soil moisture field data becomes available in the spring 2007, we will rerun the modeling effort using iTOUGH2 (Finsterle, 1999) to optimize the soil and bedrock properties to see if better matches to the field data are possible. Because of the uncertainty in some of the soil moisture measurements, we will remove the field instruments to perform recalibration tests. Based on the results of this analysis, we will further revisit the model development, calibration, and sensitivity analysis.

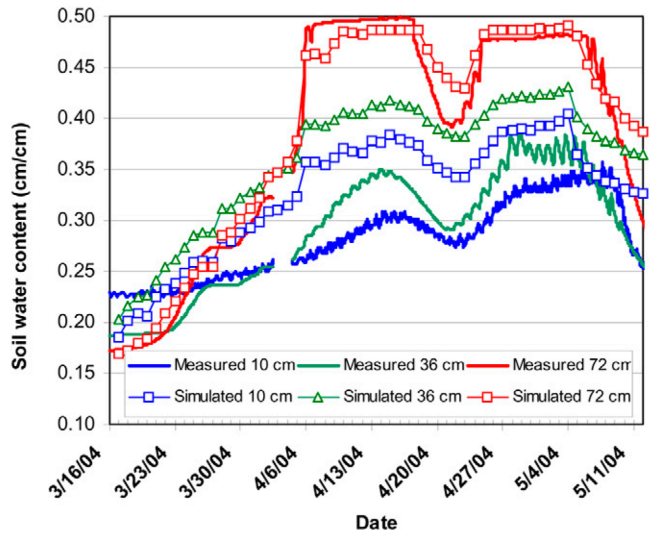

Fig. 12. Measured and simulated soil water content for 3 mo during springtime snowmelt for three soil layers.

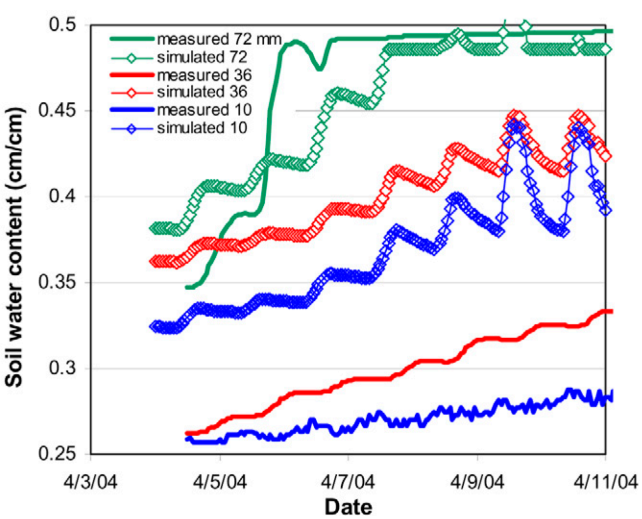

Fig. 13. Measured and simulated soil water content for the 86-cm-deep soil for 5–8 Apr. 2003 during the initiation of the snowmelt sequence.

To better understand the melt–pond–drain process, hourly simulation output was evaluated for 4 d at the beginning of snowmelt, 5 to 8 Apr. 2004 (Fig. 13). The simulation does a reasonable job of reproducing the diurnal signature of the melt–pond–drain process; however, it does not attain full saturation at 72-cm until midday on 7 April, possibly due to the heterogeneity of the snowmelt between the snow pillow and the instrumented soil pit being 10 m away. This preliminary model result will be further tested with more rigorous modeling when the field data from 2007 become available (battery failure caused loss of data in 2005 and much of 2006, although some melt data from 2006 is now being analyzed).

One hypothesis tested was that lateral flow was contributing to the drop in water content at the bedrock interface and that no infiltration into the bedrock was occurring. To test this hypothesis, vertical columns were extracted from the results of the two-dimensional model simulation with a 5% slope (illustrated in Fig. 14). One assumption in this analysis was that the instruments were on the "crest" of a local subsurface bedrock divide and that all infiltrating water was moving away from the instruments with no inflow from upgradient. Even under this assumption, there is a small decrease in water content under the melting condition that is far exceeded by the no-melt drainage seen on 20 April (Fig.

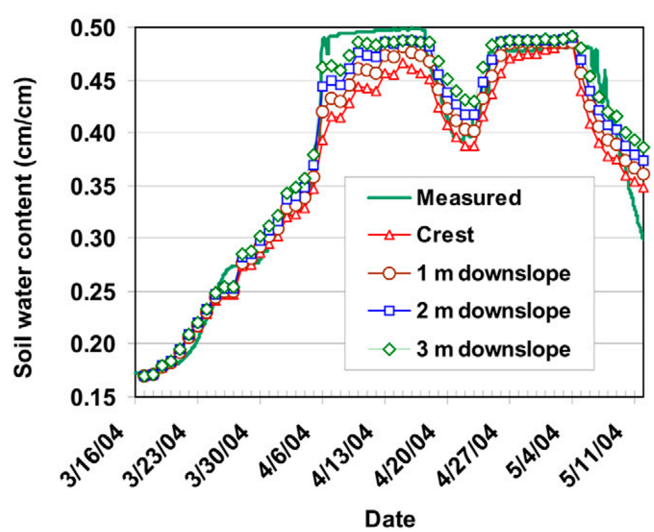

Fig. 14. Results from a two-dimensional simulation with a 5% slope.

7a). This supports the contention that field observations of local slope were not this heterogeneous. The second scenario of lateral flow away from the measurement site resulting in the decline in the soil water content (interpreted as bedrock infiltration) indicates no such result. With only 3 m of upgradient contributing area, the amount of inflow equaled the amount of outflow along the soil–bedrock interface. Field observations, including ground penetrating radar measurements (data not presented) could not identify a possible bedrock divide, which further supports the hypothesis that infiltration into the bedrock was occurring under the snowpack at the instrumented site. A two-dimensional representation of the model domain illustrating volumetric water content results for the two-dimensional simulation is shown in Fig. 15, including flux vectors indicating direction. Vertical flow still dominates at the soil–bedrock contact; however, the no-flow boundary condition at the downslope boundary is influencing the flux direction from 7 to 10 m. Although the water content continued to increase down gradient from the crest, only small changes occurred in the first meter (Fig. 14 and 15). It should be noted that the model results shown in Fig. 12 and 13 were taken from the vertical column 4 m downslope in the two-dimensional model domain. From these results, it appears that when the snowmelt rate is at or less than the bedrock permeability (which is the case for most of the snowmelt season; Fig. 4), direct infiltration into the bedrock can occur and little lateral flow exists. This would suggest that snowmelt water that reaches the nearby stream travels through the fractured granitic rock rather than overland flow or subsurface lateral flow at the soil–bedrock contact.

Summary

Soil moisture field data were collected under a melting snowpack at Gin Flat in Yosemite National Park. A conceptual model was developed that suggests that as the snow melts, it infiltrates into the soil and percolates vertically downward until it contacts the soil–bedrock interface. The best estimate of the bedrock permeability (infiltration rate under ponded conditions) at Gin Flat is 1.6 cm d^{-1}. As long as the infiltration from the melting snowpack does not exceed this, little direct runoff or near-surface underflow can be sustained (instead, the infiltrating water drains into deeper bedrock fractures and connections); once the infiltration rate (at the surface) significantly exceeds this rate, water ponds at the bedrock surface and presumably can support near-surface underflow toward local streams and meadows. As the snowpack refreezes at night, the soil-water continues to drain out of the soil profile at the bedrock permeability rate until the next morning when the snowpack again begins to melt, resulting in increases in soil-water content (the diurnal wetting and draining cycle). This cycle continues until the snowpack is gone (this assumes air temperatures cycle above and below freezing during the day). If freezing temperatures were not obtained at night then the snowpack would continue to melt and not cycle. There is the potential for some lateral flow to be occurring during this time, but not as significant as the vertical flow. Numerical modeling supports this hypothesis and generally reproduces the diurnal and seasonal signatures. Further data collection in 2007, along with additional refinement of the numerical model, will be used to refine and support the conceptual model of snowmelt and soil processes.

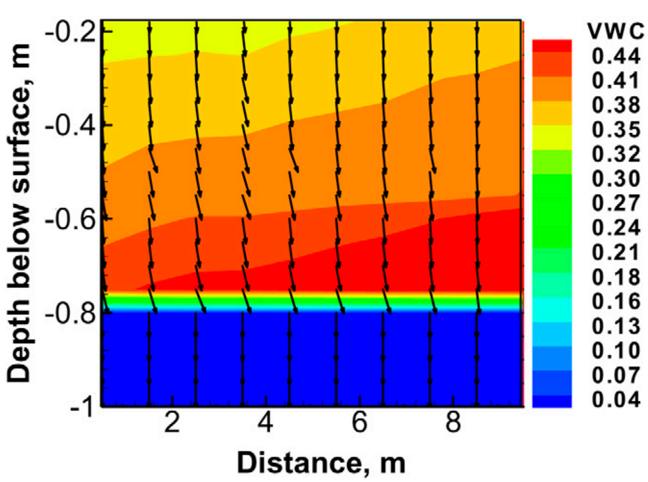

Fig. 15. Two-dimensional representation of two-dimensional simulation showing volumetric water content (VWC) and flux vector direction on 17 Apr. 2006 (horizontal to vertical was compressed 10:1; however, flux direction vectors remained 1:1).

Future Work

The preliminary modeling analysis provides insights provoking further field efforts and additional modeling analysis. The results of the model are sensitive to the fracture properties of the underlying bedrock and the timing and duration of snowmelt. Additional analysis of snowpack measurements is required to better define the snowmelt and refreezing. This upper boundary condition is the least known and may require an independent numerical model of snow accumulation, melt, and refreezing. In addition, the hydrologic properties of the bedrock are not well defined, and additional field measurements or observations are needed to provide a better rationale for the properties used in the model. New methods are being used in these remote locations to ensure battery power to the data loggers to provide more likely success in collecting soil moisture data in 2007. As mentioned earlier, the soil instruments will be removed, recalibrated, and reinstalled in a new soil pit a short distance from the old soil pit.

References

Anderson, S.P., W.E. Dietrich, D.R. Montgomery, R. Torres, M.E. Conrad, and K. Loague. 1997. Subsurface flow paths in a steep, unchanneled catchment. Water Resour. Res. 33:2637–2653.

Dane, J.H., and J.W. Hopmans. 2002. Pressure plate extractor. p. 688–690. *In* J.H. Dane and G.C. Topp (ed.) Methods of soil analysis: Part 4. Physical methods. SSSA Book Ser. 5. SSSA, Madison, WI.

Dettinger, M.D., D.R. Cayan, M.K. Meyer, and A.E. Jeton. 2004. Simulated hydrologic responses to climate variations and change in the Merced, Carson, and American River basins, Sierra Nevada, California, 1900–2099. Clim. Change 62:283–317.

Earman, S., A.P. Campbell, F.M. Phillips, and B.D. Newman. 2006. Isotopic exchange between snow and atmospheric water vapor: Estimation of the snowmelt component of greenwater recharge in the southwestern United States. J. Geophys. Res. 111:D09302, doi:10.1029/2005JD006470.

Finsterle, S. 1999. iTOUGH2 user's guide. LBNL-40040. Lawrence Berkeley National Laboratory, Berkeley, CA.

Flint, A.L., G.S. Campbell, K.M. Ellett, and C. Calissendorff. 2002. Calibration and temperature correction of heat dissipation matric potential sensors. Soil Sci. Soc. Am. J. 66:1439–1445.

Flint, A.L., and L.E. Flint. 2002a. Particle density. p. 229–240. *In* J.H. Dane and G.C. Topp (ed.) Methods of soil analysis: Part 4. Physical methods. SSSA Book Ser. 5. SSSA, Madison, WI.

Flint, A.L., L.E. Flint, J.A. Hevesi, and J.M. Blainey. 2004. Fundamental concepts of recharge in the desert southwest: A regional modeling perspective. p. 159–184. *In* J.F. Hogan, F.M. Phillips, and B.R. Scanlon (ed.) Groundwater recharge in a desert environment: The southwestern United States. Water Science and Applications Ser. Vol. 9. American Geophysical Union, Washington, DC.

Flint, L.E., and A.L. Flint. 2002b. Porosity. p. 241–254. *In* J.H. Dane and G.C. Topp (ed.) Methods of soil analysis: Part 4. Physical methods. SSSA Book Ser. 5. SSSA, Madison, WI.

Grossman, R.B., and T.G. Reinsch. 2002. Bulk density and linear extensibility. p. 201–228. *In* J.H. Dane and G.C. Topp (ed.) Methods of soil analysis: Part 4. Physical methods. SSSA Book Ser. 5. SSSA, Madison, WI

Kluitenberg, G.J. 2002. Heat capacity and specific heat. p. 1201–1208. *In* J.H. Dane and G.C. Topp (ed.) Methods of soil analysis: Part 4. Physical methods. SSSA Book Ser. 5. SSSA, Madison, WI

Kosugi, K., S. Katsura, M. Katsuyama, and T. Mizuyama. 2006. Water flow processes in weathered granitic bedrock and their effects on runoff generation in a small headwater catchment. Water Resour. Res. 42:W02414, doi:10.1029/2005WR004275.

Pruess, K., C. Oldenburg, and G. Moridis. 1999. TOUGH2 user's guide, version 2.0. LBNL-43134. Lawrence Berkeley National Laboratory, Berkeley, CA.

Schaap, M.G., F.J. Leij, and M.Th. van Genuchten. 2001. Rosetta: A computer program for estimating soil hydraulic parameters with hierarchical pedotransfer functions. J. Hydrol. 251:163–176.

Terajima, T., A. Mori, and H. Ishii. 1993. Comparative study of deep percolation amount in two small catchments in granitic mountain. (In Japanese with English abstract.). Jpn. J. Hydrol. Sci. 23(2):105–118.

Wilson, J.L., and H. Guan. 2004. Mountain-block hydrology and mountain-front recharge. p. 113–137. *In* J.F. Hogan, F.M. Phillips, and B.R. Scanlon (ed.) Groundwater recharge in a desert environment: The southwestern United States. Water Science and Applications Ser. Vol. 9. American Geophysical Union, Washington, DC.